

Matrix Production in Large Engineered Cartilage Constructs Is Enhanced by Nutrient Channels and Excess Media Supply

Robert J. Nims, MS,¹ Alexander D. Cigan, MS,¹ Michael B. Albro, PhD,^{2,3} Gordana Vunjak-Novakovic, PhD,¹ Clark T. Hung, PhD,¹ and Gerard A. Ateshian, PhD^{1,3}

Cartilage tissue engineering is a promising approach to resurfacing osteoarthritic joints. Existing techniques successfully engineer small-sized constructs with native levels of extracellular matrix (glycosaminoglycans [GAG] or collagen). However, a remaining challenge is the growth of large-sized constructs with properties similar to those of small constructs, due to consumption and transport limitations resulting in inadequate nutrient availability within the interior of large constructs. This study employed system-specific computational models for estimating glucose requirements of large constructs, with or without channels, to enhance nutrient availability. Based on glucose requirements for matrix synthesis in cartilage constructs, computational simulations were performed to identify the media volume (MV) and the number of nutrient channels (CH) needed to maintain adequate glucose levels within tissue constructs over the 3-day period between media replenishments. In Study 1, the influence of MV (5, 10, 15 mL/construct) and number of nutrient channels (CH: 0, 3, 7, 12 per construct) on glucose availability was investigated computationally for $\varnothing 10 \times 2.34$ mm cylindrical constructs. Results showed that the conventionally used MV 5 led to deleterious glucose depletion after only 40 h of culture, and that MV 15 was required to maintain sufficient glucose levels for all channel configurations. Study 2 examined experimentally the validity of these predictions, for tissue constructs cultured for 56 days. Matrix elaboration was highest in MV 15/CH 12 constructs ($21.6\% \pm 2.4\%/ww$ GAG, $5.5\% \pm 0.7\%/ww$ collagen, normalized to wet weight (ww) on day 0), leading to the greatest amount of swelling (3.0 ± 0.3 times day-0 volume), in contrast to the significantly lower matrix elaboration of conventional culture, MV 5/CH 0 ($11.8\% \pm 1.6\%/ww$ GAG and $2.5\% \pm 0.6\%/ww$ collagen, 1.6 ± 0.1 times day-0 volume). The computational analyses correctly predicted the need to increase the conventional media levels threefold to support matrix synthesis in large channeled engineered constructs. Results also suggested that more elaborate computational models are needed for accurate predictive tissue engineering simulations, which account for a broader set of nutrients, cell proliferation, matrix synthesis, and swelling of the constructs.

Introduction

OSTEoARTHRITIS (OA) IS A DEBILITATING degenerative disease that degrades the articular cartilage of diarthrodial joints, compromising its low-friction load-bearing function.¹⁻³ OA often becomes symptomatic only after large focal defects (~ 5 cm²) have appeared, eventually progressing to encompass most of the articular surface.⁴ Cartilage

tissue engineering (CTE) is a promising technique for the treatment of OA. In our vision, a tissue replacement would be cultured first *in vitro* to develop a robust native matrix before *in vivo* implantation into the large focal defects.⁵

While conventional culture techniques can successfully engineer small constructs (~ 0.1 cm²) approaching native levels of glycosaminoglycans (GAG) and collagen,⁶⁻⁸ culturing large constructs for resurfacing clinically relevant

This work was previously submitted in abstract form as follows:

Nims, R.J., Cigan, A.D., Albro, M.B., Park, D.B., Vunjak-Novakovic, G., Hung, C.T., and Ateshian, G.A. Increasing glucose availability in large engineered cartilage constructs using nutrient channels: a finite element study. Abstract presented at the International Symposium on Computer Methods in Biomechanics and Biomedical Engineering, Salt Lake City, UT, 2013. Abstract No. SS16-5.

Cigan, A.D., Nims, R.J., Albro, M.B., Quien, M.M., Atkatsch, K.M., Hung, C.T., and Ateshian, G.A. Elevated matrix production in large engineered cartilage constructs is facilitated by nutrient channels and sufficient media. Abstract presented at the Orthopaedic Research Society Meeting, New Orleans, LA, 2014. Abstract No. 0134.

¹Department of Biomedical Engineering, Columbia University, New York, New York.

²Department of Materials, Imperial College London, London, United Kingdom.

³Department of Mechanical Engineering, Columbia University, New York, New York.

defect sizes remains a challenge.⁹ Consumption by cells in the construct's peripheral regions hinders the transport of nutrients critical for matrix synthesis in the inner regions, limiting the size to which functional constructs can be grown. To overcome transport limitations, several strategies have been employed for enhancing nutrient availability. Heywood *et al.* demonstrated that increasing media volume (MV) in cultures of small [primary bovine chondrocyte]–[alginate] constructs enhanced extracellular matrix (ECM) elaboration and homogeneity.^{10,11} More recently, our laboratory and others have incorporated nutrient channels into large constructs. This reduction in nutrient path length within large constructs produced tissues with higher compressive mechanical properties and improved matrix distribution over channel-free constructs, although differences in the total matrix content were insignificant.^{12–14} Despite these advances, our limited understanding of the specific nutrient requirements for construct synthesis compromises the application of culture strategies to larger constructs. This notion is supported by the variability of media supply rates found in the literature (Table 1).^{7,11,13,15–21}

The aim of our study was to formulate and validate system-specific computational models for estimating the nutrient supplies needed to engineer large tissues, with or without nutrient channels. These models may account for system-specific ECM synthesis and nutrient consumption. This study focused specifically on the supply of glucose in the [juvenile bovine chondrocyte]–[agarose gel] CTE system. In our recent experimental study of cellular glucose consumption and

matrix synthesis in small constructs ($\varnothing 4 \times 2.34$ mm), a glucose concentration of 12.5 mM was identified as the nutrient threshold below which the ECM synthesis ceased.^{21,22} This threshold represented half the initial glucose concentration of 25 mM in standard cell culture media, suggesting that such standard conditions may easily lead to nutrient depletion in tissue engineering studies when the media/cell ratio is inadequate. Indeed, preliminary simulations conducted for this study suggested that our standard culture conditions fail to supply larger ($\varnothing 10 \times 2.34$ mm) constructs with adequate glucose levels for ECM elaboration. Consequently, placing nutrient channels into constructs would be ineffective under those conditions, potentially leading to confounding results if nutrient levels were not accounted for.

Motivated by these insights, we investigated whether computational models, informed by this critical glucose threshold and experimentally characterized glucose consumption rates, can identify adequate levels of MV per construct to ensure optimal matrix synthesis during tissue culture for a variety of channel configurations. To this end, finite element (FE) models were first used to simulate the influences of MV and nutrient channel density on the glucose concentrations within large constructs (Study 1); in this manner, the theoretical conditions required for sufficient glucose availability were identified. Informed by Study 1, large constructs were experimentally cultured for 8 weeks under these computationally predicted suboptimal and optimal conditions, and their mechanical properties and biochemical composition were assessed (Study 2).

TABLE 1. OVERVIEW OF CULTURE CONDITIONS REPORTED FOR CARTILAGE TISSUE ENGINEERING

Study	Cell type	Construct dimensions (mm)	Cells per construct (million cells per construct)	Media volume (mL per construct)	Duration (days)	Glucose Conc. (mM)	Media supply rate (mL per million cells per day)	Glucose supply rate (μ mol per million cells per day)
Buschmann ¹⁵	JBC	$\varnothing 16 \times 1$	4.0	2	1	25	0.49	12.4
Vunjak-Novakovic ¹⁶	JBC	$\varnothing 10 \times 5$	7.0	3	1	25	0.43	10.7
Obradovic ¹⁷	JBC	$\varnothing 5 \times 2$	5.0	5	3	25	0.33	8.3
Mauck ¹⁸	JBC	$\varnothing 4.67 \times 1.6$	0.3	0.5	3	25	0.59	14.6
			0.6	0.5	3	25	0.29	7.3
			1.7	0.5	3	25	0.10	2.4
Davisson ¹⁹	JBC	$\varnothing 10 \times 2$	20	12.5	3	25	0.21	5.2
Kisiday ²⁰	JBC	$40 \times 40 \times 1.6$	38.4	12	2	25	0.16	3.9
			76.8	12	2	25	0.08	1.9
Heywood ¹¹	JBC	$25 \times 50 \times 4$	25	20	3	22	0.26	5.9
			50	20	3	22	0.13	2.9
			100	20	3	22	0.07	1.5
			200	20	3	22	0.03	0.7
		$\varnothing 6 \times 4$	4.5	1.81	3	22	0.13	2.9
				3.62	3	22	0.27	5.9
				7.24	3	22	0.53	11.7
				14.48	3	22	1.07	23.4
				28.96	3	22	2.13	46.9
Hu ⁷	JBC	N/A	5.5	0.5	1	25	0.09	2.27
Buckley ¹³	ABC	$\varnothing 6 \times 4$	1.7	3.75	3	25	0.74	18.4
Nims ²¹	JBC	$\varnothing 4 \times 2.34$	0.88	0.5	3	25	0.19	4.7
This work	JBC	$\varnothing 10 \times 2.34$	11.0	5	3	25	0.15	3.8
			11.0	15	3	25	0.45	11.3

Culture conditions were used to calculate the daily media replenishment volume per million cells and the daily moles of glucose replaced per million cells.

JBC, juvenile bovine chondrocytes; ABC, adult bovine chondrocytes.

Methods

Study 1: nutrient simulations

Nutrient supply and consumption models were implemented in FEBio (www.febio.org) to simulate the glucose concentration in tissue constructs and their surrounding bath throughout a 3-day culture period.^{23,24} These models employ a multiphasic mixture framework that accounts for chemical reactions, simulating glucose transport from the bath into the construct, glucose diffusion within the construct, and glucose consumption by chondrocytes.²¹ Chondrocytes were not modeled explicitly, but their consumption of glucose was described by a sink rate uniformly distributed across the construct geometry to represent a similarly homogeneous cell-seeding density. In the standard 2-2-3-day media change schedule, the 3-day period simulated here represented the longest duration without nutrient replenishment. Based on the system-specific experimental parameters (glucose threshold and glucose consumption rate),^{21,22} simulations were performed to identify the culture conditions that prevented the glucose concentration throughout the construct from dropping below the glucose threshold for ECM synthesis.

Constructs were modeled as being suspended within a well-stirred bath, boundary conditions representative of the experimental configuration.¹⁴ The bath was modeled explicitly and well-stirred conditions were simulated using glucose diffusivity 1000 times higher than in the construct.²¹ FE model geometries and meshes (CUBIT; Sandia National Laboratory) matched the geometries of several candidate channel and bath configurations (Fig. 1): constructs ($\varnothing 10 \times 2.34$ mm) suspended within a media bath volume of 5, 10, or 15 mL (MV: 5, 10, and 15) and configured with 0, 3, 7, or 12 channels (CH: 0, 3, 7, 12), generating a total of 12 culture conditions. CH groups represent triangular packing arrangements of $\varnothing 1$ mm channels that may be inscribed symmetrically within a $\varnothing 10$ mm construct; the MV groups were selected such that the lowest (5 mL/construct) represented a typical media/cell ratio employed in CTE experiments (Table 1), while the highest (15 mL/construct) was predicted to supply adequate glucose according to the nutrient threshold. As these geometries exhibited both axial and radial symmetries, symmetrical representative regions (CH 0, 3, 12: 60° , CH 7: 30° ; all: half-thickness) were modeled with symmetry planes (zero-flux boundaries), as shown in Figure 1 (bottom).

To examine how an infinitely large (or continuous) supply of fresh media would influence construct glucose concentrations, simulations were also run with a fixed 25 mM glucose concentration prescribed at the construct surface (group MV ∞).

Glucose was modeled as an uncharged solute with a constant free diffusivity $D_0 = 9.2 \times 10^{-4} \text{ mm}^2 \cdot \text{s}^{-1}$ and mixture diffusivity $D = 8.7 \times 10^{-4} \text{ mm}^2 \cdot \text{s}^{-1}$ ²⁵; the constructs had solid volume fractions of 2%, typical of freshly cast constructs. Glucose transport and supply were related through mass balance,

$$\partial c^{\text{glc}} / \partial t - \text{div}(D \text{ grad } c^{\text{glc}}) = \hat{c}^{\text{glc}} \quad (1)$$

where c^{glc} is the glucose concentration and \hat{c}^{glc} is the glucose supply resulting from chemical reactions. A nominal construct cellularity of $60 \times 10^6 \text{ cells} \cdot \text{mL}^{-1}$ was utilized to inform the glucose consumption rates of the construct ma-

terial. To account for variability in the cell glucose consumption rates, simulations for each culture condition were based on the mean, $1.24 \times 10^{-13} \text{ mol} \cdot \text{h}^{-1} \cdot \text{cell}^{-1}$, and 95% confidence interval (CI) limits, $0.69\text{--}1.81 \times 10^{-13} \text{ mol} \cdot \text{h}^{-1} \cdot \text{cell}^{-1}$, of the glucose consumption rate for this culture system.²¹ Cellular glucose consumption was modeled according to Michaelis-Menten kinetics,

$$\hat{c}^{\text{glc}} = \frac{V_{\text{max}}^{\text{glc}} c^{\text{glc}}}{K_m + c^{\text{glc}}} \quad (2)$$

where $V_{\text{max}}^{\text{glc}}$ is the maximal glucose consumption rate of the tissue (with mean value of $2.07 \mu\text{M} \cdot \text{s}^{-1}$ and 95% CI limits

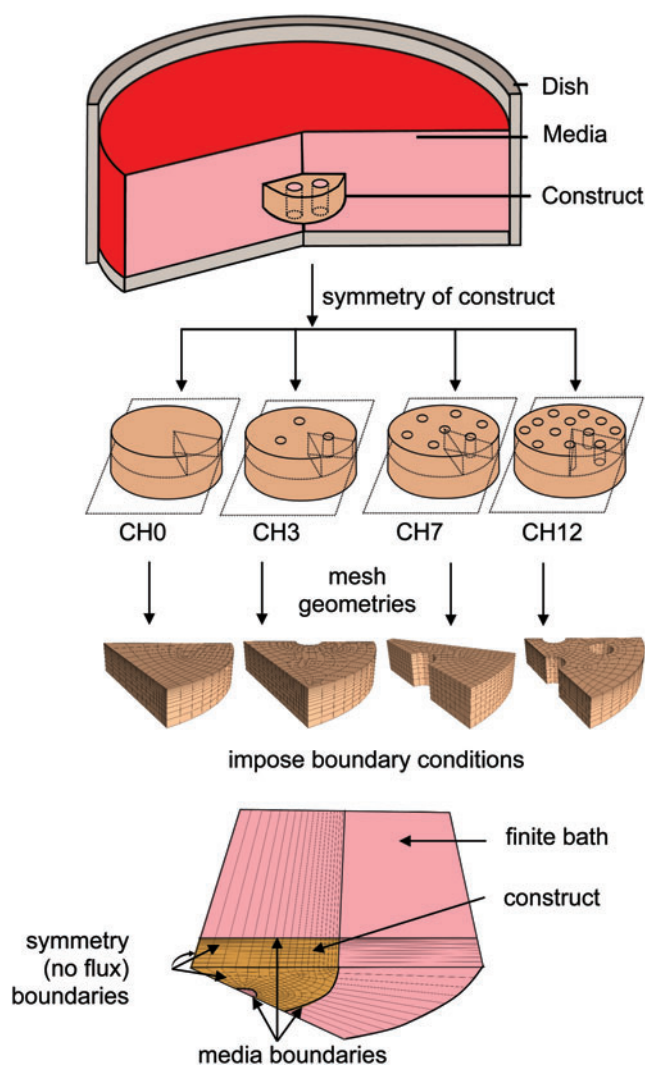


FIG. 1. Experimental configuration. Theoretical models were developed for channeled constructs suspended in a well-mixed bath. Constructs (with 0, 3, 7, and 12 channels each) were modeled according to the available symmetry (axial and radial). Models featured a finite media bath, either 5, 10, or 15 mL; constructs then had either a media bath boundary conditions (lateral, top, and channel, if present, surfaces) or no flux boundary conditions (sagittal cut edges and bottom transverse plane); as shown is CH 3/MV 5 configuration. CH, nutrient channels; MV, media volume. Color images available online at www.liebertpub.com/tec

of $1.15\text{--}3.03\ \mu\text{M}\cdot\text{s}^{-1}$) and K_m is the Michaelis constant, $0.35\ \text{mM}$.^{26,27} The initial glucose concentration in both the media and construct materials was $25\ \text{mM}$, based on high-glucose Dulbecco's modified Eagle's media (DMEM). Models simulated a 72 h period during which glucose consumption occurred in the construct and glucose transport from the surrounding bath occurred by passive diffusion through the construct. After the culture simulation, the minimum glucose concentration within the construct was determined.

Study 2: experimental culture

Cell harvesting and construct casting were performed according to previous methods.⁸ Briefly, cartilage was harvested from juvenile bovine carpometacarpal joints (local abattoir) and digested with type IV collagenase (Sigma-Aldrich) in high-glucose DMEM (Invitrogen) supplemented with 5% fetal bovine serum, amino acids, buffering agents, and 1% antibiotic-antimycotic (Invitrogen) at 37°C for 8 h with a total solution activity of $1000\ \text{U}\cdot\text{mL}^{-1}$.²⁸ Isolated primary chondrocytes were encapsulated in 2% type-VIIA agarose (Sigma-Aldrich) at a nominal density of $60\times 10^6\ \text{cells}\cdot\text{mL}^{-1}$. The cell-molten agarose mixture was cast into a custom mold (2.34 mm thick) featuring a glass slide opposite a polytetrafluoroethylene (PTFE) sheet studded with stainless steel pins arranged in the desired channel configurations of the constructs.¹⁴ Constructs ($\varnothing 10\ \text{mm}$) were cored from this cast layer with 0, 3, or 12 channels (groups: CH 0, 3, 12). The CH 7 constructs modeled computationally were omitted from experiments, as we determined that one intermediate CH group (CH 3) was sufficient to test the hypothesis. Constructs were cultured in chemically defined chondrogenic media supplemented with TGF- $\beta 3$ for the first 2 weeks.^{6,8} Media consisted of high-glucose (25 mM glucose) DMEM supplemented with sodium pyruvate ($100\ \mu\text{g}\cdot\text{mL}^{-1}$), L-proline ($50\ \mu\text{g}\cdot\text{mL}^{-1}$), 1% antibiotic-antimycotic, 100 nM dexamethasone, ITS+premix (BD Biosciences), and $173\ \mu\text{M}$ ascorbic acid 2-phosphate.²² Based on the simulation results of Study 1, constructs received 5, 10, or 15 mL of media (groups: MV 5, 10, 15) and media were replenished according to a 2-2-3-day schedule. Spent media samples were collected from each group at each media change. Constructs were cultured in a PTFE rack system, which kept them upright on their lateral sides, thus maximizing their surface area available for nutrient transport and aligning channels in the direction of media stirring.¹⁴ Media stirring was introduced by 0.8 Hz orbital shaking during culture.

Mechanical, biochemical, and histological measurements

Constructs ($n = 5$) were assessed on day 56 for mechanical properties (in unconfined compression to measure equilibrium Young's modulus, E_Y) and biochemical composition (for DNA, GAG, and collagen contents). For biomechanical assessment, construct dimensions were measured before an unconfined compression (10% specimen height) and relaxation ($\sim 11,000\ \text{s}$); E_Y was calculated from the relaxed tissue load and the undeformed construct dimensions.^{14,28} Photographs of constructs were taken to assess the degree of channel filling and images were imported into NIH ImageJ

(<http://imagej.nih.gov/ij/>) for data analysis. Day 56 channel area was normalized to day 0 area (based on $\varnothing 1\ \text{mm}$ channel) to measure percentage channel filling. For biochemical assessment, constructs were weighed (day 56 wet weight, D56ww) and digested with the proteinase K reagent²⁹ before assaying for DNA (PicoGreen Assay, Invitrogen; 7.7 pg DNA/cell ratio^{30,31}), GAG (dimethylmethylene blue dye-binding assay, DMMB³²), and orthohydroxyproline (OHP) content (OHP assay³³; 7.64 collagen/OHP mass ratio³⁴). Briefly, GAG in the proteinase K digests was directly assayed through DMMB, and OHP was measured after acid hydrolysis of the digests. The hydrolyzed sample was dried and resuspended before reacting with chloramine T and an aldehyde/perchloric acid solution.³³ The construct swelling ratio (SR) was calculated by normalizing D56ww by the ww of constructs on day 0 (D0ww). Biochemical content was normalized to both D0ww and D56ww. Spent media samples were assayed for glucose (Amplex Red Assay; Invitrogen), GAG, and OHP. Samples for histological characterization were fixed (5% acetic acid, 3.7% formaldehyde, 70% ethanol solution),³⁵ dehydrated in successively concentrated ethanol solutions, embedded in paraffin, and sectioned to $7\ \mu\text{m}$ slices. Following paraffin removal, sections were stained with either Safranin O to qualitatively assay the negative charges of GAG or Picrosirius red to qualitatively assay for collagen.³⁶

Statistical analyses

Day 56 experimental measures were assessed with a two-way ANOVA ($\alpha = 0.05$); factors were CH, MV, and their interaction (CH \times MV). Tukey's HSD *post hoc* comparisons were used to compare differences between groups ($p \leq 0.05$). Data are presented as mean \pm standard deviation.

Results

Study 1: nutrient simulations

Glucose consumption by the cells within constructs caused the projected glucose concentrations to drop throughout the construct and bath substantially below the initial concentration (25 mM), with glucose levels varying spatially throughout the constructs (Fig. 2). Channels enabled the maintenance of more homogeneous glucose concentrations, whereas channel-free constructs exhibited large concentration gradients between the construct surface and center. The temporal evolution of the minimum glucose concentration (at the construct center) is presented in Figure 3, based on average cellular consumption rate. These results show that at low media supply (MV 5), glucose concentrations were below the 12.5 mM threshold for all CH configurations as early as 40 h for CH 0 and 50 h for CH 12 after medium change. Conversely, for MV 15, glucose concentrations exceeded the threshold level throughout the 72 h of culture for all CH groups. The MV 10 group maintained the glucose levels slightly above the threshold for all CH groups at 72 h. However, when examining the effect of cell consumption rate variability (Fig. 4), results show that the MV 10 groups mostly straddle the critical threshold concentration, especially for CH 0 and 3. Only the MV 15 group consistently exceeded the glucose concentration threshold for all channel configurations.

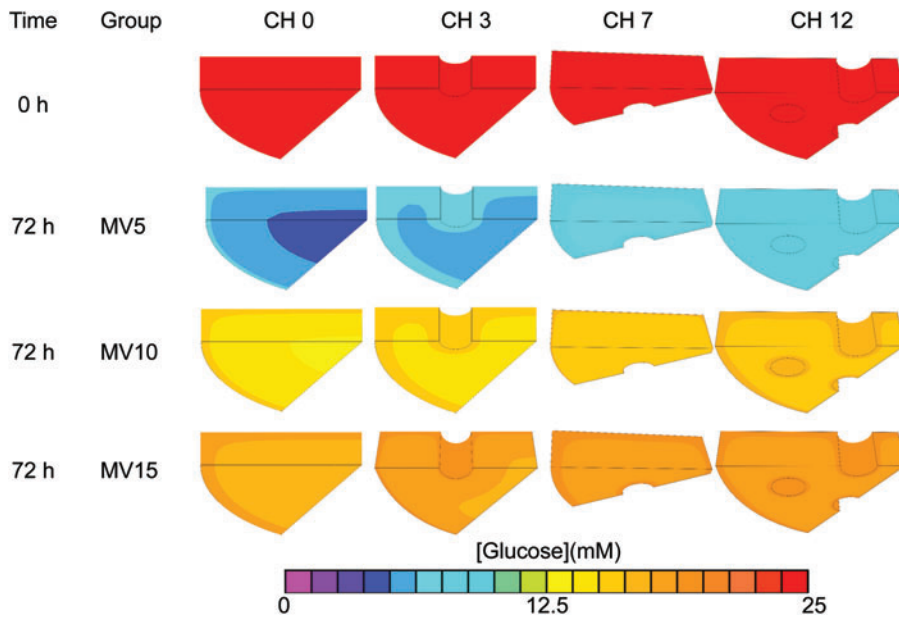


FIG. 2. Model-predicted influence of channels (0, 3, 7, and 12 channels per construct) and media volume (MV 5, 10, 15 mL per construct) on glucose profiles within constructs after 72 h of culture. Color images available online at www.liebertpub.com/tec

On average, the minimum construct glucose concentration increased by 8.4 mM between the MV 5 and 10 groups, and by 2.7 mM between the MV 10 and 15 groups (Fig. 3). For a given MV, the minimum glucose concentration within the construct increased by an average of 0.6 mM between each CH level (i.e., 0–3, 3–7, or 7–12). The MV ∞ group further elevated minimum glucose concentrations; the minimum construct glucose concentration of the CH 0, 3, 7, and 12 constructs was 23.2, 23.4, 23.8, and 24.4 mM, respectively, at 72 h. From these predictions, it became evi-

dent that increasing MV led to diminishing returns in glucose availability; a MV of 15 was sufficient to elevate all CH groups with 95% confidence above the 12.5 mM threshold (Fig. 4). Therefore, this MV was selected as the highest MV for experimental culture.

Study 2: experimental culture

After 56 days, all groups had similar $E_Y \sim 304 \pm 97$ kPa (Fig. 5A; $p > 0.13$). SR (Fig. 5B) was significantly influenced

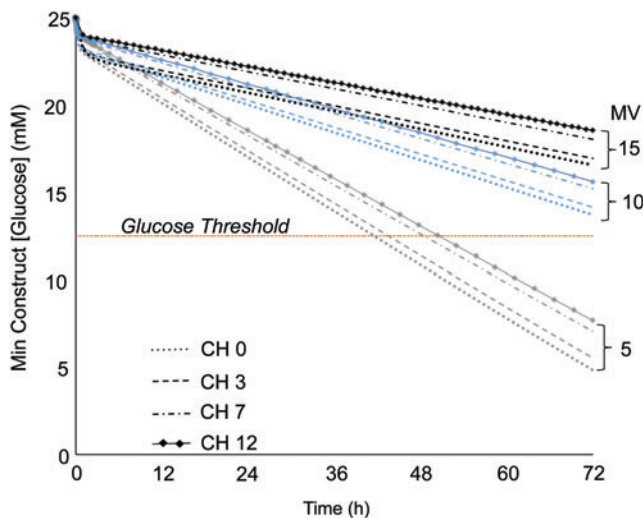


FIG. 3. Theoretical predictions of the minimum glucose concentration within the construct over the 72 h culture period. *Trend lines* represent the mean level of glucose consumption for the different channel configurations (*dotted line*, CH 0; *dashed line*, CH 3; *dot-dashed line*, CH 7; *line-through dots*, CH 12) and media supplementation volumes (MV levels indicated on right). *Horizontal dashed line* denotes the critical glucose threshold for matrix synthesis (12.5 mM). Color images available online at www.liebertpub.com/tec

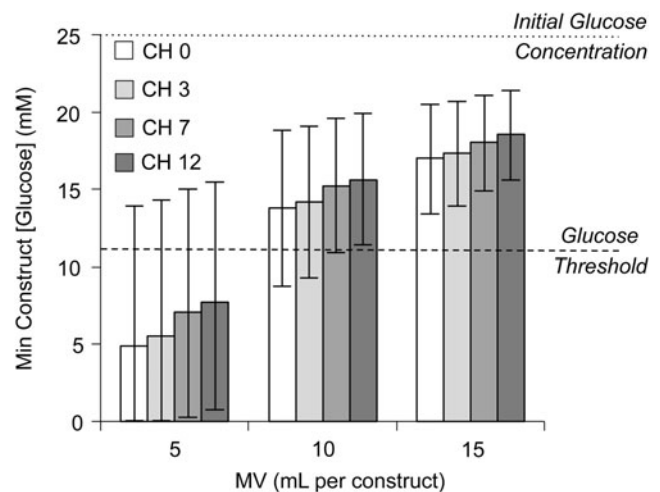
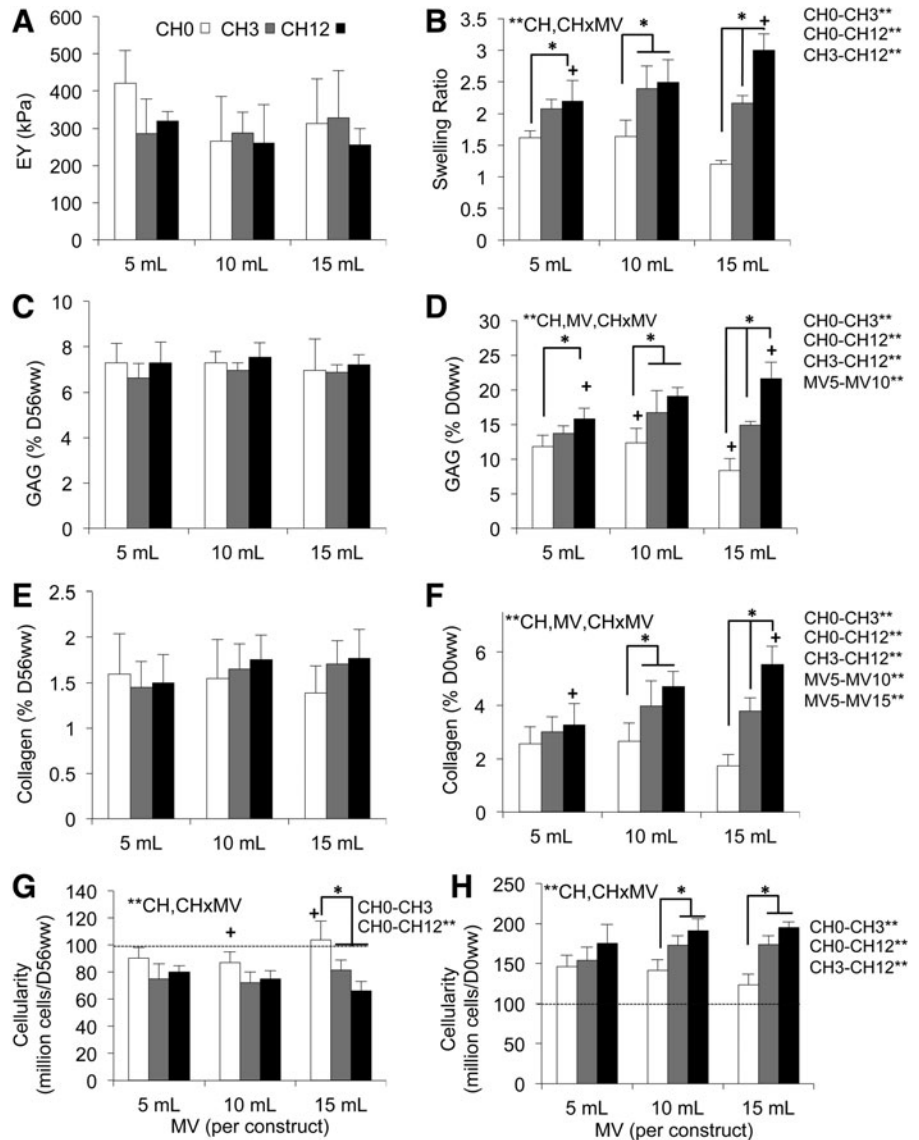


FIG. 4. Theoretical predictions of the minimum glucose concentration within the construct after the 72 h culture period. Bar value represents mean glucose consumption level; high error bar represents the low 95% confidence interval (CI) consumption level; low error bar represents the high 95% CI consumption level. *Dotted line* denotes initial glucose concentration (25 mM); *dashed line* denotes the critical glucose threshold for matrix synthesis (12.5 mM).

FIG. 5. Mechanical and biochemical construct properties (day 56), (A) E_Y (kPa), (B) swelling ratio (SR), (C) glycosaminoglycans (GAG) (%/D56ww), (D) GAG (%/D0ww), (E) collagen (%/D56ww), (F) collagen (%/D0ww), (G) cell density (cell [D56 mL]⁻¹), (H) cell density (cell [D0 mL]⁻¹). *Significance of CH within given MV ($p < 0.05$); +significance of CH for different MV ($p < 0.05$); **significance of indicated factors (CH, MV, and/or CH×MV or groups; $p < 0.05$). Dashed lines (G, H) depict mean day 0 cellularity (99.4 million cells [D0 mL]⁻¹).



by CH ($p < 0.001$), but not MV ($p = 0.059$). In the extreme instance, the CH 12 group swelled 3.00 ± 0.26 times the day-0 ww when cultured in MV 15; CH 0 constructs at this same MV remained near day-0 dimensions ($SR = 1.20 \pm 0.07$; Fig. 6). Due to this disparity of construct swelling, biochemical normalizations were performed with respect to both D56ww and D0ww to examine the composition of the final constructs and total matrix deposition, respectively. Relative to D56ww, neither GAG (Fig. 5C; $7.1\% \pm 0.7\%$; $p > 0.12$) nor collagen (Fig. 5E; $1.6\% \pm 0.3\%$; $p > 0.35$) significantly differed due to effects of MV or CH. Relative to D0ww, the GAG content was significantly influenced by CH (Fig. 5D; $p < 0.001$), MV ($p = 0.006$), and CH×MV ($p < 0.001$); most notably, in the MV 15 group, CH 12 had $2.6\times$ the GAG content of CH 0. For all CH values, MV 10 had more GAG than MV 5 ($p = 0.004$). Similarly, when collagen mass was normalized to D0ww (Fig. 5F), CH ($p < 0.001$), MV ($p = 0.014$), and CH×MV ($p < 0.001$) significantly influenced collagen content. For all CH values, MV 10 had more collagen than MV 5 ($p = 0.014$). CH ($p < 0.001$) but not MV ($p \geq 0.23$) influenced the cell

density (as normalized by both D56ww and D0ww; Fig. 5G, H, respectively). All groups increased in cellularity from day-0 values ($99.4 \pm 1.1 \times 10^6$ cells·mL⁻¹).

The loss of matrix macromolecules into the culture media is shown in Table 2. The average daily release of GAG into the culture media varied with CH ($p < 0.001$), MV ($p < 0.001$), and CH×MV ($p = 0.048$); specifically, CH 12 released more GAG than CH 0 ($p = 0.003$) and CH 3 ($p = 0.012$); and MV 15 released more GAG than MV 10 ($p = 0.015$), which released more GAG than MV 5 ($p = 0.003$). Collagen release varied with CH ($p = 0.005$) and MV ($p < 0.001$) but not CH×MV ($p = 0.29$); CH 12 released more collagen than CH 0 ($p = 0.011$), and MV 10 and 15 released more collagen than MV 5 ($p = 0.045$ and $p < 0.001$, respectively).

Glucose concentrations in spent media are presented separately for media collected after a 2-day (GLU D2) or 3-day (GLU D3) period in the (2-2-3-day) weekly media replenishment schedule. GLU D2 varied with CH ($p < 0.001$) and MV ($p < 0.001$) but not with CH×MV ($p = 0.91$); GLU

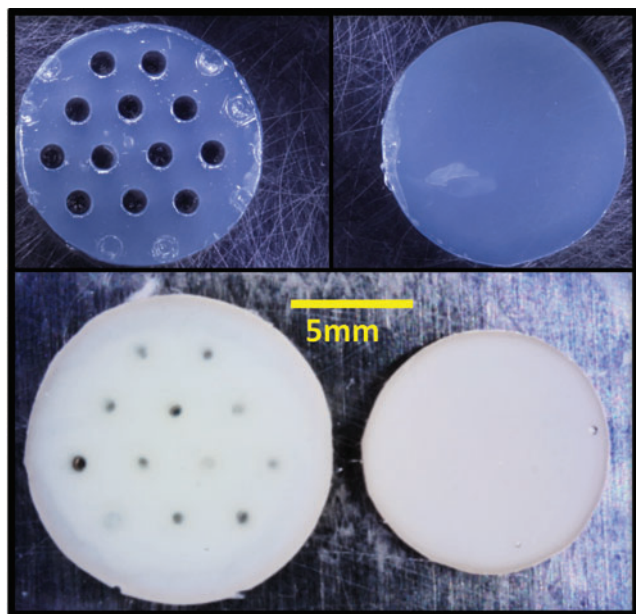


FIG. 6. Effect of excess medium on construct swelling. Gross morphological differences in swelling of the experimental MV 15 group between CH 12 (left) and CH 0 (right) groups between freshly cast agarose (top) and mature D56 constructs (bottom). Scale bar, 5 mm. Color images available online at www.liebertpub.com/tec

D3 varied with MV ($p < 0.001$) but was not different between CH groups ($p = 0.24$). For GLU D2 and GLU D3, MV 15 had a higher glucose concentration than MV 5 ($p < 0.001$ and $p = 0.001$, respectively) and MV 10 ($p < 0.001$ and $p < 0.001$, respectively); and MV 10 was elevated over MV 5 ($p < 0.001$ and $p = 0.046$, respectively). For GLU D2, CH 12 maintained a higher glucose concentration over CH 0 ($p = 0.010$).

Histological analyses (Fig. 7) of the groups display intense Safranin O staining throughout the constructs with a denser staining profile in the MV 15 groups compared to MV 5; the CH 0 group also had a lower intensity band (Fig. 7, A1 arrow) between the more intense center and periphery. Collagen staining was more diffuse than GAG, with a higher intensity band present midway between the center and periphery in the CH 0 constructs (Fig. 7, A2 arrow). This apparent inverse relationship between GAG and collagen content was also apparent in a thin boundary layer around each of the channels (Fig. 7, B arrows).

Channel filling (Table 3) was significantly higher in the CH 12 group compared to CH 3 ($p = 0.017$), while MV had no significant effect ($p = 0.104$).

Discussion

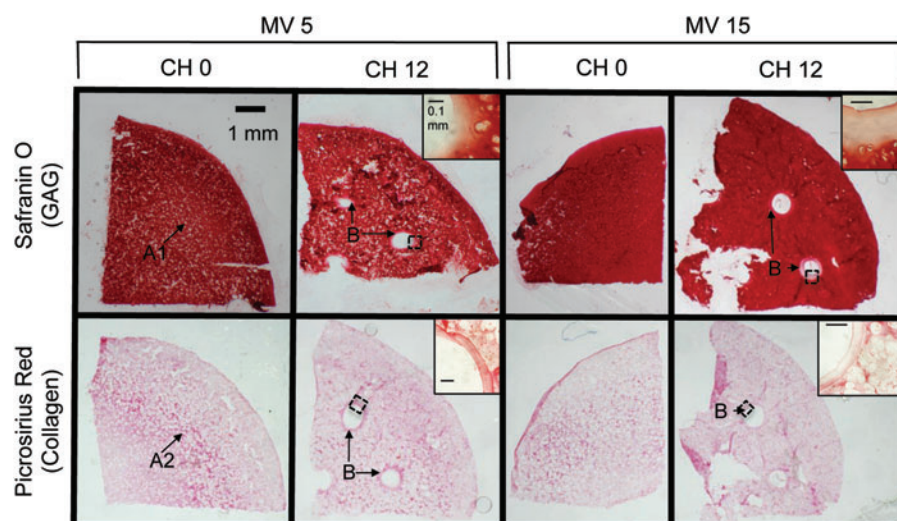
The objective of this study was to formulate and validate system-specific computational models for estimating nutrient supplies needed to culture large engineered tissues, with or without nutrient channels. Based on our recent investigations, which reported the glucose threshold necessary for matrix synthesis and a representative glucose consumption rate in our CTE system,^{21,22} we focused on the availability of glucose as an essential nutrient. Predictions from the

TABLE 2. RELEASE OF GAG AND COLLAGEN INTO CULTURE MEDIUM AND FINAL GLUCOSE CONCENTRATION

MV CH	5			10			15		
	0	3	12	0	3	12	0	3	12
GAG release (SD) ($\mu\text{g} \cdot \text{mL}^{-1} \cdot \text{day}^{-1}$)	408 ^{AC} (125)	431 ^{AC} (147)	484 ^{AC} (172)	509 ^{AC} (165)	567 ^{AC} (227)	663 ^B (286)	587 ^{AC} (207)	636 ^{BC} (273)	856 ^B (426)
Collagen release (SD) ($\mu\text{g} \cdot \text{mL}^{-1} \cdot \text{day}^{-1}$)	185 (83)	253 (145)	243 (99)	244 (152)	344 (188)	435 (226)	322 (137)	408 (219)	495 (149)
Glucose D2 (SD) (mM)	12.6 (1.2)	12.7 (2.8)	11.3 (0.8)	16.7 (1.4)	14.5 (2.2)	13.0 (2.2)	19.0 (2.3)	17.7 (2.8)	17.5 (2.4)
Glucose D3 (SD) (mM)	9.5 ^{AC} (2.3)	8.3 ^A (1.4)	11.1 ^{AC} (4.8)	16.4 ^{BC} (1.7)	12.8 ^{AC} (1.8)	14.4 ^{ABC} (4.1)	20.1 ^B (3.2)	17.3 ^B (1.8)	14.9 ^{ABC} (4.3)

Glucose concentration is separated into 2-day (D2) and 3-day (D3) groups. Groups with differing superscripts statistically differ ($p < 0.05$). GAG, glycosaminoglycans.

FIG. 7. Histological analysis of CH 0 and 12 and MV 5 and 15 samples. GAG (Safranin O) and collagen (Picrosirius red) staining in the CH 0 and 12 groups for the MV 5 or MV 15 mL media supplementation volumes. Representative perichannel images are included (*inset*) for the salient CH 12 images. *Arrow A*: banding in GAG (A1) and collagen (A2) in CH 0 group. *Arrow B*: channel GAG and collagen. Scale bar 1 mm for bulk construct images and 100 μ m for enhanced *inset* image. Color images available online at www.liebertpub.com/tec



simulations indicated that standard media/cell ratios used in studies of smaller constructs (Table 1) may be inadequate for culturing larger constructs, and that channel incorporation alone would not ameliorate this nutrient depletion. According to the models, a higher MV would be required for maximal matrix elaboration and greater effectiveness of nutrient channels, as related to glucose.

With this guidance, constructs (CH 0, 3, 12) were experimentally cultured at standard (MV 5 per $\varnothing 10 \times 2.34$ mm construct) or elevated (MV 10 and 15) MV, to investigate the validity of computational predictions. Prior investigations of this culture system with constructs of this size or smaller have demonstrated that chondrocytes maintain their morphology throughout the construct.^{14,37–40} When examining total matrix elaboration, as represented by D0ww-normalized compositional measures in Figure 5, increasing MV produced significantly greater ECM deposition (GAG and collagen, Fig. 5D, F); these quantitative measures were further corroborated qualitatively by the more intense Safranin O staining of the MV 15 groups, compared to MV 5 (Fig. 7). Nutrient channels further increased ECM deposition, with the most dramatic CH-induced enhancements evident in the presence of high MV (Fig. 5D, F). These experimental results supported the model predictions that standard media/cell levels produced suboptimal matrix synthesis and that channels at standard media levels do not demonstrate much effectiveness for larger constructs.

While the GAG and collagen content normalized by D0ww illustrated differences in ECM synthesis as a function of MV and CH, these differences were not evident when

TABLE 3. CHANNEL FILLING AFTER 56 DAYS IN CULTURE FOR CH 3 AND 12 GROUPS

MV	CH	
	3 ^a	12 ^a
5	69 ± 9	82 ± 5
10	79 ± 13	86 ± 4
15	71 ± 13	77 ± 8

Percentage channel filling is evaluated relative to day 0 channel area 0.785 mm² (based on a $\varnothing 1$ mm channel).

^aDenotes differences between indicated groups ($p < 0.05$).

using the more conventional normalization to ww on the last day of culture (D56ww). Indeed, although greater matrix synthesis was observed with increasing MV and CH, E_Y showed no significant differences among the groups (Fig. 5A), presumably because their variable swelling (Fig. 5B) maintained the fixed-charge density of GAGs at a nearly uniform level (Fig. 5C).

In prior studies, we have noted that our CTE system is able to produce GAG at native levels ($\sim 6\%$ ww for immature bovine cartilage), but that collagen remains significantly below native values ($\sim 10\%$ ww), as was observed here ($\sim 7\%$ D56ww GAG in Fig. 5C and $\sim 1.5\%$ D56ww collagen in Fig. 5E). Interestingly, day 0 normalizations suggest that the amount of collagen actually synthesized (almost $\sim 6\%$ D0ww in Fig. 5F for the MV 15/CH 12 group) could produce weight ratios closer to native levels, were it not for the substantial swelling (Fig. 5B) driven by the Donnan osmotic pressure from charged GAG.^{41–43} These results support the value of strategies using exogenous treatments such as lysyl oxidase to strengthen the collagen network by increasing collagen cross-link precursors and to prevent the swelling evident in this study.⁴⁴

In prior studies of this model system,⁴⁵ it had been suggested that the higher deposition of GAG might inhibit collagen deposition, possibly due to a steric effect. Histological stains from this study support this hypothesis (Fig. 7), especially around channel edges, where a greater proportion of synthesized GAGs may diffuse into the channel due to their natural time constant for binding with the scaffold,²¹ allowing for a more intense ring of deposited collagen. This hypothesis had previously motivated alternative strategies for enhancing collagen deposition by using chondroitinase ABC to enzymatically remove GAG and quell construct swelling.⁴⁶

The amount of glucose available in the culture media was adjusted by changing the MV per construct instead of modifying the glucose concentration. This choice was motivated by the desire to maintain the glucose concentration at the standard 25 mM of high-glucose DMEM and the concern that large changes in concentration might produce confounding effects due to alterations in osmolality and pH.^{10,47}

Another potential concern is that large numbers of channels may compromise the construct mechanical

integrity, possibly leading to stress concentrations and cracking under loading. No cracking was observed during mechanical testing on day 56, although the possibility that such damage may occur at physiological load magnitudes should not be discounted. In native cartilage, the network of channels that irrigates the tissue during development and through adolescence eventually disappears. A process whereby channels completely occlude at the time of construct maturation would be similarly beneficial; by day 56 of this study, channels filled by approximately 75% (Table 3), suggesting that complete filling may occur at a later time point. Depending on the level of elaboration of functional properties in the construct, ensuring free flow of media in the channels for longer culture durations may require periodic material removal. Alternatively, strategies may be needed, such as the injection of cell-seeded agarose, to completely fill channels before implantation.

The computational model employed herein builds from earlier efforts to model engineered cartilage nutrient consumption^{25,47–51} and serves as a critical step to develop system-specific models for assessing the culture of the characterized CTE systems. Models may similarly guide future studies by identifying the most promising experimental culture conditions for a given construct geometry and cell density, eliminating less promising ones, and reducing the need for labor- and cost-intensive experimental parametric studies.

While the model here provided insight on the culture of large constructs, subsequent models may be considerably improved in future implementations. Under the current framework, the model predicted that all CH groups within the MV 15 group should produce similar matrix levels. Experimental results, however, demonstrated that for MV 15 groups, CH was a significant factor influencing the ECM content, suggesting that additional factors may need to be modeled to account for these observations.^{25,49} Channels also increased the total construct cell content (Fig. 5H), implying that channels in constructs may act both to increase nutrient availability and enhance the synthesis capacity of the constructs. Thus, cellular proliferation may need to be incorporated into future growth models when simulating multiple weeks of culture.^{52,53} In addition, early matrix synthesis models implicated oxygen as a limiting nutrient,^{17,49,50} and recently, our laboratory has shown that active TGF- β binds extensively to the native ECM suggesting potential transport limitations within engineered constructs.⁵⁴ Therefore, the transport, binding, consumption, and biosynthetic influence of oxygen and TGF- β may need to be included explicitly in future models. Construct swelling, resulting from ECM synthesis and Donnan osmotic pressure, may also need to be modeled to better reproduce observed phenomena (Figs. 5B, H, and 6). With these improved models, it will become possible to optimize the placement and density of channels for growing full-sized engineered cartilage layers, recognizing the competition between increasing the number of channels to enhance nutrient access and reducing the number of cells available for matrix synthesis.

In summary, computational models are becoming increasingly valuable tools for designing effective culture conditions for engineering large tissue constructs. This study specifically addressed the amount of glucose in our [juvenile bovine chondrocyte]–[agarose gel] CTE system, as a wide

range of media and glucose supply rates have been employed in prior studies (Table 1), illustrating the lack of consensus on adequate amounts of this fundamental nutrient. It was found computationally that conventional culture conditions provide inadequate glucose levels for culturing larger constructs, obviating the benefits of nutrient channels. Experimental results demonstrated that significantly enhanced matrix deposition in channeled constructs could be achieved when using higher MV supplementation (Figs. 5D, F, and 6). This agreement between model prediction and subsequent experimentation encourages further development and validation of predictive models, including models that account for a broader set of nutrients, cell proliferation, matrix synthesis, and swelling of the constructs. These more sophisticated models may be subjected to more stringent quantitative validations of a variety of measures, including matrix composition, mechanical properties, and dimensional changes.

Acknowledgment

Research reported in this publication was supported by the National Institute of Arthritis and Musculoskeletal and Skin Diseases of the National Institutes of Health under Award Numbers R01AR060361, R01AR046568, T32AR059038, 2R01DE016525, and 2P41EB002520. The content is solely the responsibility of the authors and does not necessarily represent the official views of the National Institutes of Health.

Disclosure Statement

The authors have no competing financial interests.

References

1. Krishnan, R., Kopacz, M., and Ateshian, G.A. Experimental verification of the role of interstitial fluid pressurization in cartilage lubrication. *J Orthop Res* **22**, 565, 2004.
2. Mow, V.C., Ateshian, G.A., and Spilker, R.L. Biomechanics of diarthrodial joints: a review of twenty years of progress. *J Biomech Eng* **115**, 460, 1993.
3. Stockwell, R.A. *Biology of Cartilage Cells*. Cambridge: Cambridge University Press, 1979.
4. Moisio, K., Eckstein, F., Chmiel, J.S., Guermazi, A., Prasad, P., Almagor, O., Song, J., Dunlop, D., Hudelmaier, M., Kothari, A., and Sharma, L. Denuded subchondral bone and knee pain in persons with knee osteoarthritis. *Arthritis Rheum* **60**, 3703, 2009.
5. Hunziker, E.B. Articular cartilage repair: basic science and clinical progress. A review of the current status and prospects. *Osteoarthritis Cartilage* **10**, 432, 2002.
6. Byers, B.A., Mauck, R.L., Chiang, I.E., and Tuan, R.S. Transient exposure to transforming growth factor beta 3 under serum-free conditions enhances the biomechanical and biochemical maturation of tissue-engineered cartilage. *Tissue Eng Part A* **14**, 1821, 2008.
7. Hu, J.C., and Athanasiou, K.A. A self-assembling process in articular cartilage tissue engineering. *Tissue Eng* **12**, 969, 2006.
8. Lima, E.G., Bian, L., Ng, K.W., Mauck, R.L., Byers, B.A., Tuan, R.S., Ateshian, G.A., and Hung, C.T. The beneficial effect of delayed compressive loading on tissue-engineered cartilage constructs cultured with Tgf-Beta3. *Osteoarthritis Cartilage* **15**, 1025, 2007.

9. Hung, C.T., Lima, E.G., Mauck, R.L., Takai, E., LeRoux, M.A., Lu, H.H., Stark, R.G., Guo, X.E., and Ateshian, G.A. Anatomically shaped osteochondral constructs for articular cartilage repair. *J Biomech* **36**, 1853, 2003.
10. Heywood, H.K., Bader, D.L., and Lee, D.A. Glucose concentration and medium volume influence cell viability and glycosaminoglycan synthesis in chondrocyte-seeded alginate constructs. *Tissue Eng* **12**, 3487, 2006.
11. Heywood, H.K., Sembi, P.K., Lee, D.A., and Bader, D.L. Cellular utilization determines viability and matrix alginate constructs in chondrocyte-seeded alginate constructs. *Tissue Eng* **10**, 1467, 2004.
12. Bian, L., Angione, S.L., Ng, K.W., Lima, E.G., Williams, D.Y., Mao, D.Q., Ateshian, G.A., and Hung, C.T. Influence of decreasing nutrient path length on the development of engineered cartilage. *Osteoarthritis Cartilage* **17**, 677, 2009.
13. Buckley, C.T., Thorpe, S.D., and Kelly, D.J. Engineering of large cartilaginous tissues through the use of microchanneled hydrogels and rotational culture. *Tissue Eng Part A* **15**, 3213, 2009.
14. Cigan, A.D., Nims, R.J., Albro, M.B., Vunjak-Novakovic, G., Hung, C.T., and Ateshian, G.A. Nutrient channels and stirring enhanced the composition and stiffness of large cartilage constructs. *J Biomech* **47**, 3847, 2014.
15. Buschmann, M.D., Gluzband, Y.A., Grodzinsky, A.J., Kimura, J.H., and Hunziker, E.B. Chondrocytes in agarose culture synthesize a mechanically functional extracellular matrix. *J Orthop Res* **10**, 745, 1992.
16. Vunjak-Novakovic, G., Freed, L.E., Biron, R.J., and Langer, R. Effects of mixing on the composition and morphology of tissue-engineered cartilage. *AIChE J* **42**, 850, 1996.
17. Obradovic, B., Carrier, R.L., Vunjak-Novakovic, G., and Freed, L.E. Gas exchange is essential for bioreactor cultivation of tissue engineered cartilage. *Biotechnol Bioeng* **63**, 197, 1999.
18. Mauck, R.L., Seyhan, S.L., Ateshian, G.A., and Hung, C.T. Influence of seeding density and dynamic deformational loading on the developing structure/function relationships of chondrocyte-seeded agarose hydrogels. *Ann Biomed Eng* **30**, 1046, 2002.
19. Davisson, T., Kunig, S., Chen, A., Sah, R.L., and Ratcliffe, A. Static and dynamic compression modulate matrix metabolism in tissue engineered cartilage. *J Orthop Res* **20**, 842, 2002.
20. Kisiday, J., Jin, M., Kurz, B., Hung, H., Semino, C., Zhang, S., and Grodzinsky, A.J. Self-assembling peptide hydrogel fosters chondrocyte extracellular matrix production and cell division: implications for cartilage tissue repair. *Proc Natl Acad Sci U S A* **99**, 9996, 2002.
21. Nims, R.J., Cigan, A.D., Albro, M.B., Hung, C.T., and Ateshian, G.A. Synthesis rates and binding kinetics of matrix products in engineered cartilage constructs using chondrocyte-seeded agarose gels. *J Biomech* **47**, 2165, 2014.
22. Cigan, A.D., Nims, R.J., Albro, M.B., Esau, J.D., Dreyer, M.P., Vunjak-Novakovic, G., Hung, C.T., and Ateshian, G.A. Insulin, ascorbate, and glucose have a much greater influence than transferrin and selenous acid on the in vitro growth of engineered cartilage in chondrogenic media. *Tissue Eng Part A* **19**, 1941, 2013.
23. Ateshian, G.A., Nims, R.J., Maas, S., and Weiss, J.A. Computational modeling of chemical reactions and interstitial growth and remodeling involving charged solutes and solid-bound molecules. *Biomech Model Mechanobiol* **13**, 1105, 2014.
24. Maas, S.A., Ellis, B.J., Ateshian, G.A., and Weiss, J.A. FEBio: finite elements for biomechanics. *J Biomech Eng* **134**, 011005, 2012.
25. Sengers, B.G., van Donkelaar, C.C., Oomens, C.W., and Baaijens, F.P. Computational study of culture conditions and nutrient supply in cartilage tissue engineering. *Biotechnol Prog* **21**, 1252, 2005.
26. Michaelis, L., Menten, M.L., Johnson, K.A., and Goody, R.S. The original Michaelis constant: translation of the 1913 Michaelis-Menten paper. *Biochemistry* **50**, 8264, 2011.
27. Windhaber, R.A.J., Wilkins, R.J., and Meredith, D. Functional characterisation of glucose transport in bovine articular chondrocytes. *Pflugers Archiv* **446**, 572, 2003.
28. Mauck, R.L., Soltz, M.A., Wang, C.C., Wong, D.D., Chao, P.H., Valhmu, W.B., Hung, C.T., and Ateshian, G.A. Functional tissue engineering of articular cartilage through dynamic loading of chondrocyte-seeded agarose gels. *J Biomech Eng* **122**, 252, 2000.
29. Hollander, A.P., Heathfield, T.F., Webber, C., Iwata, Y., Bourne, R., Rorabeck, C., and Poole, A.R. Increased damage to type Ii collagen in osteoarthritic articular cartilage detected by a new immunoassay. *J Clin Invest* **93**, 1722, 1994.
30. Kim, Y., Sah, R., Doong, J., and Grodzinsky, A. Fluorometric assay of DNA in cartilage explants using Hoechst 33258. *Anal Biochem* **76**, 168, 1988.
31. McGowan, K.B., Kurtis, M.S., Lottman, L.M., Watson, D., and Sah, R.L. Biochemical quantification of DNA in human articular and septal cartilage using Picogreen and Hoechst 33258. *Osteoarthritis Cartilage* **10**, 580, 2002.
32. Farndale, R.W., Buttle, D.J., and Barrett, A.J. Improved quantitation and discrimination of sulphated glycosaminoglycans by use of dimethylmethylene blue. *Biochim Biophys Acta* **883**, 173, 1986.
33. Stegemann, H., and Stalder, K. Determination of hydroxyproline. *Clin Chim Acta* **18**, 267, 1967.
34. Nimni, M.E. Seminars in arthritis and rheumatism: collagen: structure, functions, and metabolism in normal and fibrotic tissues. *Semin Arthritis Rheum* **13**, 1, 1983.
35. Lin, W., Shuster, S., Maibach, H.I., and Stern, R. Patterns of hyaluronan staining are modified by fixation techniques. *J Histochem Cytochem* **45**, 1157, 1997.
36. Kelly, T.A., Ng, K.W., Wang, C.C., Ateshian, G.A., and Hung, C.T. Spatial and temporal development of chondrocyte-seeded agarose constructs in free-swelling and dynamically loaded cultures. *J Biomech* **39**, 1489, 2006.
37. Benya, P.D., and Shaffer, J.D. Dedifferentiated chondrocytes reexpress the differentiated collagen phenotype when cultured in agarose gels. *Cell* **30**, 215, 1982.
38. Aydelotte, M.B., and Kuettner, K.E. Differences between sub-populations of cultured bovine articular chondrocytes. I. Morphology and cartilage matrix production. *Connect Tissue Res* **18**, 205, 1988.
39. Lee, D.A., Noguchi T., Frean, S.P., Lees, P., and Bader, D.L. The influence of mechanical loading on isolated chondrocytes seeded in agarose constructs. *Biorheology* **37**, 149, 2000.
40. Dimicco, M.A., Kisiday J.D., Gong, H., and Grodzinsky, A.J. Structure of pericellular matrix around agarose-embedded chondrocytes. *Osteoarthritis Cartilage* **15**, 1207, 2007.
41. Eisenberg, S.R., and Grodzinsky, A.J. Swelling of articular cartilage and other connective tissues: electromechanochemical forces. *J Orthop Res* **3**, 148, 1985.

42. Lai, W.M., Hou, J.S., and Mow, V.C. A Triphasic theory for the swelling and deformation behaviors of articular cartilage. *J Biomech Eng* **113**, 245, 1991.
43. Mow, V.C., Ateshian, G.A., Lai, W.M., and Gu, W.Y. Effects of fixed charges on the stress-relaxation behavior of hydrated soft tissues in a confined compression problem. *Int J Solids Structures* **35**, 4945, 1998.
44. Athens, A.A., Makris, E.A., and Hu, J.C. Induced collagen cross-links enhance cartilage integration. *PLoS One* **8**, e60719, 2013.
45. Bian, L., Crivello, K.M., Ng, K.W., Xu, D., Williams D.Y., Ateshian, G.A., and Hung, C.T. Influence of temporary chondroitinase ABC-induced glycosaminoglycan suppression on maturation of tissue-engineered cartilage. *Tissue Eng Part A* **15**, 2065, 2009.
46. O'Connell, G.D., Nims, R.J., Green, J., Cigan, A.D., Ateshian, G.A., and Hung, C.T. Time and dose-dependent effects of chondroitinase ABC on growth of engineered cartilage. *Eur Cell Mater* **27**, 312, 2014.
47. Zhou, S., Cui, Z., and Urban, J.P. Nutrient gradients in engineered cartilage: metabolic kinetics measurement and mass transfer modeling. *Biotechnol Bioeng* **101**, 408, 2008.
48. Lin, T.H., Jhang, H.Y., Chu, F.C., and Chung, C.A. Computational modeling of nutrient utilization in engineered cartilage. *Biotechnol Prog* **29**, 452, 2013.
49. Nikolaev, N.I., Obradovic, B., Versteeg, H.K., Lemon, G., and Williams, D.J. A validated model of Gag deposition, cell distribution, and growth of tissue engineered cartilage cultured in a rotating bioreactor. *Biotechnol Bioeng* **105**, 842, 2010.
50. Obradovic, B., Meldon, J.H., Freed, L.E., and Vunjak-Novakovic, G. Glycosaminoglycan deposition in engineered cartilage: experiments and mathematical model. *AIChE J* **46**, 1860, 2000.
51. Galban, C.J., and Locke, B.R. Effects of spatial variation of cells and nutrient and product concentrations coupled with product inhibition on cell growth in a polymer scaffold. *Biotechnol Bioeng* **64**, 633, 1999.
52. Lemon, G., and King, J.R. Multiphase modelling of cell behaviour on artificial scaffolds: effects of nutrient depletion and spatially nonuniform porosity. *Math Med Biol* **24**, 57, 2007.
53. Sengers, B.G., Heywood H.K., Lee, D.A., Oomens, C.W., and Bader, D.L. Nutrient utilization by bovine articular chondrocytes: a combined experimental and theoretical approach. *J Biomech Eng* **127**, 758, 2005.
54. Albro, M.B., Nims R.J., Cigan, A.D., Yeroushalmi, K.J., Alliston, T., Hung, C.T., and Ateshian, G.A. Accumulation of exogenous activated TGF- β in the superficial zone of articular cartilage. *Biophys J* **104**, 1794, 2013.

Address correspondence to:

Gerard A. Ateshian, PhD

Department of Mechanical Engineering

Columbia University

500 West 120th St.

Mail Code 4703

New York, NY 10027

E-mail: ateshian@columbia.edu

Received: July 29, 2014

Accepted: December 16, 2014

Online Publication Date: April 3, 2015